20th IMEKO TC10 Conference
28-29 September 2026 | Lisbon | Portugal

20th IMEKO TC10 Conference
*"Measurement for Diagnostics, Optimization and Control to Support Competitiveness and Innovation"*
Lisbon, Portugal, September 28–29, 2026

# Data-driven feedforward iterative tuning for MLPM with position-dependent nonlinearities

Qin Guangyi[1], Song Shuo[1], Dong Yue[1], Li Li[1]

[1] *Center of Ultra-precision Optoelectronic Instrument Engineering, Harbin Institute of Technology, Harbin, China, 21b901033@stu.hit.edu.cn, 23b901017@stu.hit.edu.cn, ydonghit@hit.edu.cn, hitlili@hit.edu.cn*

***Abstract*** **– To address spatial nonlinear coupling and position-dependent additive and multiplicative disturbances in Magnetically Levitated Planar Motor (MLPM) caused by decoupling mismatch, this paper proposes a data-driven position-dependent nonlinear feedforward iterative tuning method. Unlike conventional polynomial feedforward approaches, the proposed rational feedforward controller uses its numerator to compensate additive disturbances and system modes, and its denominator to handle multiplicative disturbances. Comparative experiments show that the proposed method accurately compensates both disturbance types over the full stroke, effectively overcoming the performance degradation of conventional feedforward in thrust ripple regions, and significantly improving global dynamic tracking accuracy.**

***Keywords – MLPM, feedforward iterative tuning, position-dependent disturbances.***

## I. INTRODUCTION

Magnetically levitated planar motors (MLPMs) are widely used in high-precision positioning systems such as lithography machines, scanning probes, and microscopes [1]. They enable multi-degree-of-freedom (DOF) motion without stacked structures and can operate in vacuum environments [2], avoiding friction, contamination, and error accumulation. However, practical systems still suffer from DOF coupling, position-dependent modeling errors, and inaccurate current allocation, which significantly degrade performance [3, 4].

Due to position-dependent gains and gravity-compensation-induced disturbances, MLPMs cannot be accurately modeled as linear time-invariant (LTI) systems [5]. Conventional feedforward control typically uses constant gains based on velocity and acceleration [6], which is inadequate when strong spatial variation exists, since the required compensation changes with position.

To improve tracking performance, data-driven methods have been widely studied. Iterative learning control (ILC) is effective for repetitive disturbances [7], but its learning signal is strictly trajectory-dependent, leading to poor generalization when the reference changes [8]. Parameterized feedforward iterative tuning methods extend this idea by optimizing controller parameters for different trajectories [9, 10], but most approaches still rely on constant-gain structures derived from rigid-body assumptions. Without explicitly embedding position dependence, achieving uniformly good performance over the full workspace remains difficult [11]. Therefore, designing a nonlinear decoupling strategy that combines the learning capability of ILC with the generalization ability of parameterized feedforward control remains an open challenge.

This paper proposes a data-driven position-dependent nonlinear feedforward iterative tuning method for MLPMs. Unlike polynomial feedforward approaches, the proposed rational feedforward controller uses its numerator to compensate system modes and additive disturbances, and its denominator to handle multiplicative disturbances. The model parameters are directly learned from iterative error data to compensate spatial nonlinearities.

The remainder of this paper is organized as follows. Section II introduces the MLPM system and control architecture, and describes its position-dependent nonlinear characteristics. Section III presents the proposed method in detail. Section IV provides the experimental setup and comparative results. Section V concludes the paper.

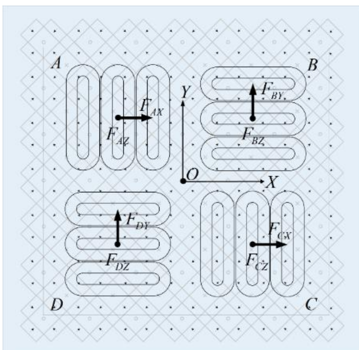


*Fig. 1. Simplified structure of the magnetically levitated planar stage.*

## II. PROBLEM FORMULATION

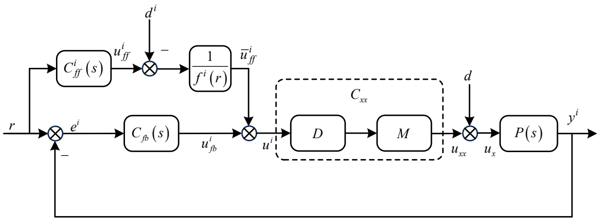


*Fig. 2. System control block diagram*

### A. MLPM control system

As shown in Fig. 1, the MLPM mainly consists of a stator with a two-dimensional Halbach array and a mover with a coil array. The multi-degree-of-freedom (DOF) motion of the mover is achieved by independently controlling the currents in each coil, forming a typical multi-input multi-output (MIMO) system. High-precision control of MLPMs usually relies on model-based decoupling strategies, aiming to decompose the coupled six-DOF dynamics into six independent single-input single-output (SISO) systems.

The control framework of the MLPM is illustrated in Fig. 2. Here, $e^i$ is the tracking error at *i*-th iteration, $r$ the reference trajectory, $y^i$ is the measured position, $C_{fb}(s)$ is the feedback controller, $C_{ff}^i(s)$ is the feedforward controller, $f^i(r)$ and $d^i$ are utilized to compensate for multiplicative and additive disturbances, $\boldsymbol{D}$ is the current allocation matrix, $\boldsymbol{M}$ is the physical actuation matrix.

### B. Decoupling mismatch and spatial nonlinear disturbances

Define the coupling matrix as $\boldsymbol{C} = \boldsymbol{MD}$. Ideally, if the allocation matrix perfectly matches the true actuation system, then $\boldsymbol{C}(y) = \boldsymbol{I}_{6\times 6}$, yielding complete decoupling: $\boldsymbol{F}(t) = \boldsymbol{I}_{6\times 6}\boldsymbol{u}_{fb}(t)$ . In practice, due to higher-order magnetic harmonics and manufacturing tolerances, the actuation matrix exhibits strong position dependence, leading to $\boldsymbol{C}(y) \neq \boldsymbol{I}_{6\times 6}$. For example, the force along the X-axis can be expressed as

$$u_x(t) = C_{xx}(y)u_{fb}(t) + \sum_{j\neq x} C_{xj}(y)u_{fb,j}(t), \quad (1)$$

This mismatch introduces significant nonlinear disturbances, which can be categorized as follows:

Position-dependent multiplicative disturbance: Associated with the diagonal term $C_{xx}(y)$. The effective force gain is no longer constant but varies with position, resulting in nonlinear variations in the forward-loop gain.

Position-dependent additive disturbance: Associated with the off-diagonal terms. In active magnetic levitation systems, a large static force command ( $u_{fb,z} \approx mg$ ) is required along the Z-axis to maintain levitation. This command couples into horizontal axes (e.g., X-axis) via $C_{xz}(y)$, producing parasitic forces:

$$F_{add,x}(y) \approx C_{xz}(y)u_{fb,z}(t), \quad (2)$$

Since parameters such as $C_{xx}(y)$ and $C_{xz}(y)$ strongly depend on the spatial position, conventional fixed-parameter linear controllers cannot achieve effective compensation over the entire motion range. Therefore, it is essential to use measured position data and computed feedback control signals within a data-driven, position-dependent nonlinear feedforward iterative tuning framework to accurately compensate for spatial nonlinear disturbances caused by imperfect decoupling.

## III. DESIGN OF THE PROPOSED METHOD

### A. Feedforward controller parameterization

From Fig. 2, the reference-trajectory feedforward control signal can be parameterized as:

$$u_{ff}^* = \boldsymbol{\lambda\theta}^* + \boldsymbol{\gamma\vartheta}^* \quad (3)$$

where $\boldsymbol{\lambda}, \boldsymbol{\gamma}$ and $\boldsymbol{\theta}^*, \boldsymbol{\vartheta}^*$ are basis function vectors and corresponding parameter vectors. $\mathcal{L}\left(\boldsymbol{\lambda\theta}^*\right) = P^{-1}(s)r(s)$, $\mathcal{L}(\cdot)$ is the Laplace transform, $\boldsymbol{\gamma\vartheta}^* = -d$ .

The multiplicative disturbance compensation term can be parameterized as:

$$f(r) = 1 + \boldsymbol{\rho\sigma}^* \quad (4)$$

where $\boldsymbol{\rho}$ is the basis function vector, $\boldsymbol{\sigma}^*$ is the corresponding parameter vector.

Therefore, the feedforward controller $u_{ff}^i$ can be written as:

$$u_{ff}^i = \frac{\boldsymbol{\lambda\theta}^i + \boldsymbol{\gamma\vartheta}^i}{1 + \boldsymbol{\rho\sigma}^i} \quad (5)$$

where $\boldsymbol{\theta}^i, \boldsymbol{\vartheta}^i, \boldsymbol{\sigma}^i$ are parameters to be tuned.

### B. Data-driven IFFT

Define $\boldsymbol{\delta}^i = \left[\left(\boldsymbol{\theta}^i\right)^{\mathrm{T}}, \left(\boldsymbol{\vartheta}^i\right)^{\mathrm{T}}, \left(\boldsymbol{\sigma}^i\right)^{\mathrm{T}}\right]^{\mathrm{T}}$ and $\boldsymbol{\delta}^* = \left[\left(\boldsymbol{\theta}^*\right)^{\mathrm{T}}, \left(\boldsymbol{\vartheta}^*\right)^{\mathrm{T}}, \left(\boldsymbol{\sigma}^*\right)^{\mathrm{T}}\right]^{\mathrm{T}}$, to make $\boldsymbol{\delta}^i$ approach $\boldsymbol{\delta}^*$, the data-driven IFFT method is utilized. From Fig. 2, the

$e^i(s)$ can be expressed as:

$$e^i(s) = G^i(s)\mathcal{L}\left(\left[\boldsymbol{\lambda}, \boldsymbol{\gamma}, -\bar{u}_{ff}\boldsymbol{\rho}\right]\right)\left(\boldsymbol{\delta}^* - \boldsymbol{\delta}^i\right) \quad (6)$$

where $G^i(s) = 1/\left(C_{ff}^i(s) + C_{fb}(s)\right)$.

Therefore, the data-driven IFFT method is proposed as:

$$\boldsymbol{\delta}^{i+1} = \boldsymbol{\delta}^i + \boldsymbol{L}^i\boldsymbol{E}^i \quad (7)$$

where $\boldsymbol{L}^i = \left(\left(\boldsymbol{Z}^i\right)^{\mathrm{T}}\boldsymbol{Z}^i\right)^{-1}\left(\boldsymbol{Z}^i\right)^{\mathrm{T}}$, $\boldsymbol{Z}^i$ is the lifted form of $G^i(s)\mathcal{L}\left(\left[\boldsymbol{\lambda}, \boldsymbol{\gamma}, -\bar{u}_{ff}\boldsymbol{\rho}\right]\right)$, $\boldsymbol{E}^i$ is the lifted form of $e^i(t)$.

## IV. EXPERIMENTAL RESULTS

### A. *Experimental setup*

The MLPM used in the experiments is shown in Fig. 3. The mover consists of 12 coils, while the stator is a two-dimensional Halbach permanent magnet array. Horizontal position is measured using laser triangulation sensors, and vertical position is measured using eddy-current sensors. All subsequent experiments are conducted along the X-axis of the motion platform. The laser triangulation sensor has a resolution of 12 μm, and the control system operates at a sampling frequency of 5 kHz.

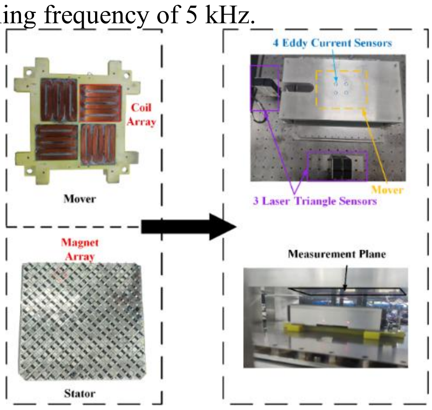


*Fig. 3. MLPM used in the experiments*

Fig. 4 shows the tracking error in the constant-velocity phase at a velocity of 0.1 m/s. It can be seen that due to the presence of multiplicative and additive disturbances, the error exhibits significant fluctuations. To obtain the frequency components, a fast Fourier transform (FFT) is performed on this constant-velocity phase. The results show that the dominant frequencies are at $f_n = 2.8571\text{Hz}$, thus the following basis functions are selected:

$$\boldsymbol{\rho} = \boldsymbol{\gamma} = \left[\sin(\omega_n r), \cos(\omega_n r), \sin(2\omega_n r), \cos(2\omega_n r), \sin(4\omega_n r), \cos(4\omega_n r)\right]$$

$$\boldsymbol{\lambda} = [A, v]$$

where $\omega_n = 2\pi f_n / 0.1$, $A$ and $v$ are reference acceleration and velocity, respectively.

A fourth-order S-curve trajectory is adopted, as shown in Fig. 5. To validate the effectiveness of the proposed method, comparisons are conducted with acceleration feedforward and combined velocity–acceleration feedforward approaches.

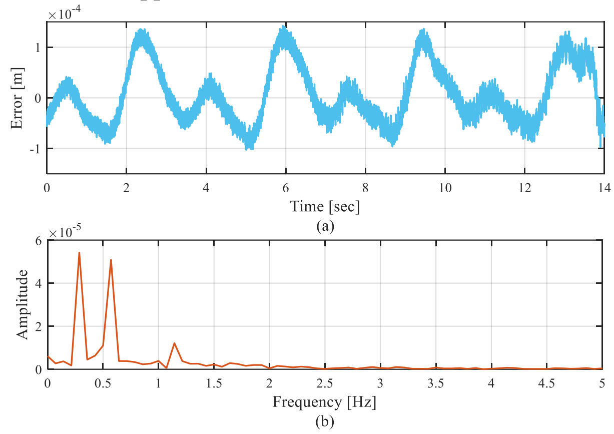


*Fig. 4. (a) The error in the constant-velocity phase at 0.1 m/sec (b) The FFT of that error*

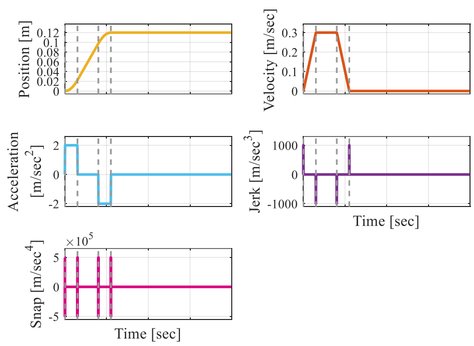


*Fig. 5. Schematic diagram of the reference trajectory*

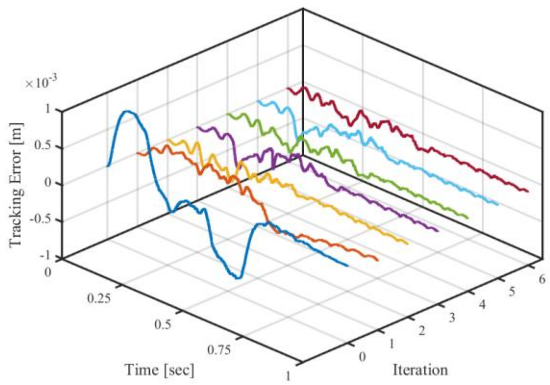


*Fig. 6. Tracking errors over iterations under the proposed method*

### B. *Tracking performance*

Fig. 6 shows the tracking error over iterations using the proposed method. The error decreases rapidly within the first three iterations, indicating fast initial convergence. After about five iterations, the algorithm converges, and the dynamic error over the entire stroke is significantly reduced and flattened. This demonstrates that the proposed approach can efficiently learn and compensate spatial position-dependent disturbances, greatly improving tracking accuracy. Fig. 7 compares the tracking errors of pure mass feedforward, mass–damping feedforward, and the proposed method at the 6th iteration. Pure mass feedforward leads to large dynamic errors (over $5\times10^{-4}$ m) due to inertia-only compensation. Mass–damping feedforward reduces the error but still shows peaks around 0.25 s and 0.5 s because constant gains cannot handle position-dependent effects. In contrast, the proposed method significantly improves performance, with errors tightly bounded across all motion phases due to accurate compensation of spatial disturbances.

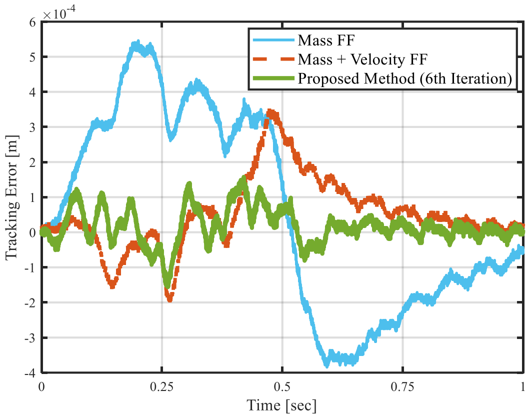


*Fig. 7. Tracking errors under different methods*

## V. CONCLUSION

This paper proposes a data-driven position-dependent rational feedforward iterative tuning strategy to compensate for spatial nonlinearities in MLPMs. The numerator of the rational feedforward controller compensates additive disturbances and system modes, while the denominator handles position-dependent multiplicative gain variations. The parameters are learned directly from measured errors, overcoming the limitations of constant-gain feedforward. Experiments show convergence within six iterations and significant improvement in tracking accuracy over the full stroke.

Future work will extend the approach to full six-DOF control and investigate multi-axis high-speed coupling dynamics.

## VI. ACKNOWLEDGMENTS

This work was supported in part by the National Natural Science Foundation of China under Grant 52105546, and in part by the Heilongjiang Postdoctoral Fund under Grant LBH-Z21154 and Grant LBH-TZ2314.

## REFERENCES

[1] Kim, W.; Trumper, D. L.: High-precision magnetic levitation stage for photolithography, Precision Engineering, Vol. 22., No. 2., 1998, pp. 66–77.

[2] Jansen, J. W.; van Lierop, C. M. M.; Lomonova, E. A.; Vandenput, A. J. A.: Modeling of magnetically levitated planar actuators with moving magnets, IEEE Transactions on Magnetics, Vol. 43., No. 1., 2007, pp. 15–25.

[3] Ou, T.; Hu, C.; Zhu, Y.; Zhang, M.: Generation mechanism and decoupling strategy of coupling effect in maglev planar motor, IEEE/ASME Transactions on Mechatronics, Vol. 28., No. 2., 2023, pp. 781–791.

[4] Broens, Y.; Butler, R.: On improved commutation for moving-magnet planar actuators, IEEE Control Systems Letters, Vol. 7., 2023, pp. 2593–2598.

[5] Rovers, J. M. M.; Jansen, J. W.; Lomonova, E. A.: Multiphysical analysis of moving-magnet planar motor topologies, IET Electric Power Applications, Vol. 7., No. 1., 2013, pp. 42–50.

[6] Heertjes, M.; Hennekens, D.; Steinbuch, M.: MIMO feed-forward design in wafer scanners using a gradient approximation-based algorithm, Control Engineering Practice, Vol. 18., No. 5., 2010, pp. 495–506.

[7] Bristow, D. A.; Tharayil, M.; Alleyne, A. G.: A survey of iterative learning control, IEEE Control Systems Magazine, Vol. 26., No. 3., 2006, pp. 96–114.

[8] Blanken, L.; Oomen, T.: Multivariable iterative learning control design procedures: From decentralized to centralized, illustrated on an industrial printer, IEEE Transactions on Control Systems Technology, Vol. 28., No. 4., 2020, pp. 1534–1541.

[9] Jiang, Y.; Zhu, Y.; Yang, K.; Hu, C.; et al.: A data-driven iterative decoupling feedforward control strategy with application to an ultraprecision motion stage, IEEE Transactions on Industrial Electronics, Vol. 62., No. 1., 2015, pp. 620–627.

[10] Li, M.; Mao, C.; Zhu, Y.; Yang, K.; et al.: Data-based iterative dynamic decoupling control for precision MIMO motion systems, IEEE Transactions on Industrial Informatics, Vol. 16., No. 3., 2020, pp. 1668–1676.

[11] de Rozario, R.; Oomen, T.; Steinbuch, M.: Iterative learning control and feedforward for LPV systems: Applied to a position-dependent motion system, Proceedings of the American Control Conference (ACC), 2017, pp. 3518–3523.